Optics Communications 395 (2017) 24–28

Contents lists available at ScienceDirect

Optics Communications

journal homepage: www.elsevier.com/locate/optcom

Mechanically induced strong red emission in samarium ions doped piezoelectric semiconductor CaZnOS for dynamic pressure sensing and imaging

Wei Wang [a,b,1], Dengfeng Peng [b,1], Hanlu Zhang [b], Xiaohong Yang [a,*,2], Caofeng Pan [b,*,2]

[a] The Chongqing City Key Laboratory of Optoelectronic Functional Materials, Optical Engineering Key Lab, Chongqing Normal University, Chongqing 400047, China

[b] Beijing Institute of Nanoenergy and Nanosystems Chinese Academy of Sciences, Beijing 100083, China

ARTICLE INFO

Article history:
Received 29 December 2015
Received in revised form
1 March 2016
Accepted 16 March 2016
Available online 29 March 2016

Keywords:
Mechanoluminesense
Piezo-photonics
Dynamic pressure sensingand imaging

ABSTRACT

Piezoelectric semiconductor with optical, electrical and mechanical multifunctions has great potential applications in future optoelectronic devices. The rich properties and applications mainly encompass the intrinsic structures and their coupling effects. Here, we report that lanthanide ions doped piezoelectric semiconductor CaZnOS:Sm^{3+} showing strong red emission induced by dynamic mechanical stress. Under moderate mechanical load, the doped piezoelectric semiconductor exhibits strong visible red emission to the naked eyes even under the day light. A flexible dynamic pressure sensor device is fabricated based on the prepared CaZnOS:Sm^{3+} powders. The mechanical-induced emission properties of the device are investigated by the optical fiber spectrometer. The linear characteristic emissions are attributed to the $^4G_{5/2}\rightarrow{}^6H_{5/2}$ (566 nm), $^4G_{5/2}\rightarrow{}^6H_{7/2}$ (580–632 nm), $^4G_{5/2}\rightarrow{}^6H_{9/2}$ (653–673 nm) and $^4G_{5/2}\rightarrow{}^6H_{11/2}$ (712–735 nm) f–f transitions of Sm^{3+} ions. The integral emission intensity is proportional to the value of applied pressure. By using the linear relationship between integrated emission intensity and the dynamic pressure, the real-time pressure distribution is visualized and recorded. Our results highlight that the incorporation of lanthanide luminescent ions into piezoelectric semiconductors as smart materials could be applied into the flexible mechanical-optical sensor device without additional auxiliary power, which has great potential for promising applications such as mapping of personalized handwriting, smart display, and human machine interface.

© 2016 Elsevier B.V. All rights reserved.

1. Introduction

Piezoelectric semiconductors, i.e., ZnO, GaN, CdS, and ZnS etc. have been widely studied during the past decade because of their rich physics and widespread applications in photonics, electronics, sensors, and energy harvest [1–3]. By using the two-way coupling effect between their instinct, piezoelectricity and photoexcitation properties, the mechanical stimulation can induce piezoelectric potential which has the capability to improve the optoelectronic performance of the materials and devices. For instance, ZnO and GaN show a remarkably mechanical-induced enhancement of electroluminescence which has enable them to be used in the pressure-sensor for static pressure mapping [4–6]. On the other hand, mechanical induced light emission in piezoelectric materials has aroused great interest for their great importance in smart and energy-saving mechanical–optical–electric devices [7–15]. Recently, the doped piezoelectric semiconductors ZnS:Mn^{2+}, ZnS:Cu^{2+}, ZnS:Al^{3+}/Cu^{2+}, ZnS:Mn^{2+}/Cu^{2+}, ZnS:Al^{3+}/Mn^{2+}/Cu^{2+}, and CaZnOS:Mn^{2+}/Cu^{+} showing strong light emission directly activated by mechanical stimuli without additional auxiliary power, have been demonstrated their state-of-the-art applications in wide areas such as, light sources, displays and dynamic pressure sensor for mapping personalized handwriting [11,12,16,17]. Despite these attractions, the stress activated luminescence discovered in the piezoelectric semiconductors is generally restricted to transitional metal activators such as Mn^{2+} and Cu^{2+} ions. Lanthanide ions represent another large family of luminescent activators characterized by large stokes shift and sharp emission bandwidth and show abundant of luminescent transitions [18]. Recently, mechanically-induced emissions (MIE) have been observed from lanthanide ions, e.g. praseodymium ions doped (Ca,Ba)TiO_3 and samarium ions doped $Sr_{n+1}Sn_nO_{3n+1}$ perovskite systems [9,14]. However these materials belong to insulating dielectrics rather then piezoelectric semiconductors and could not

* Corresponding authors.
E-mail addresses: y6928@cqnu.edu.cn (X. Yang), cfpan@binn.cas.cn (C. Pan).
[1] Authors contributed equally to this work.
[2] Present address: No. 37, University City Road, Shapingba District, Chongqing 401331, China.

http://dx.doi.org/10.1016/j.optcom.2016.03.046
0030-4018/© 2016 Elsevier B.V. All rights reserved.

meet the integrated applications of the future piezoelectric semiconductor devices.

CaZnOS is an attractive piezoelectric semiconductor material with a direct band gap of ~3.7 eV comparable to that of the piezosemiconductive ZnS (3.67 eV), and high piezoelectric constant, d_{33} =38 pm V^{-1}, which is four times larger than that of ZnS (8 pm V^{-1}) [19,20]. What's more, the advantages of this material also include the mechanical and chemical stabilities, cost effective elements and easy substitution of various metal ions for Ca^{2+} and Zn^{2+} for achieving luminescence [13,21,22]. As the good host material, CaZnOS piezoelectric semiconductor is expected to show mechanical-induced emission by incorporating of lanthanide ions. In this work, we reported the strong visible emission of Sm^{3+}-doped CaZnOS piezoelectric semiconductor under mechanical stress. A flexible dynamic pressure sensor device is fabricated based on the doped powder samples. The correlation between emission intensity and dynamic pressure applied under the device is studied, showing linear intensity response to the applied dynamic pressure.

2. Experimental

Doped CaZnOS powder samples are prepared by solid-state reaction at high temperature. The starting materials are analytical grade $CaCO_3$ (99.99%, Aladdin), ZnS (99.99%, Aladdin), and Sm_2O_3 (99.99%). The powder mixtures are fired in molybdenum crucibles at 1100 °C for 4 h in a horizontal tube furnace under a flowing Ar atmosphere. The crystalline phase of the powders is examined by X-ray diffraction (XRD) θ–2θ scan with Cu-Kα radiation using philips X'PertPW-3040 diffractometer. The morphology and the elemental components of the phosphors are studied by field-emission scanning electron microscopy (FESEM) (FEI QUAANTA FEG 450) equipped with energy dispersive X-Ray spectroscopy (EDX) (EDAX TEAM EDS). For MIE properties measurement, the CaZnOS:Sm^{3+} particles are collected by further grinding and screening. The synthesized MIE phosphors are ultrasonically dispersed in methyl methacrylate (PMMA) (at the weight ratio of 1:1), followed by a rapid transfer onto a 5×5 cm^2 sized poly ethylene terephthalate with a thermoplastic ethylene-vinyl acetate copolymer (PET-EVA) thin film and its edges are enclosed by using a rectangular frame mold. After the solidification of PMMA, a flat lamina of CaZnOS:Sm^{3+} phosphors with great uniformity are deposited on the film. Finally, the film is covered by another piece of PET-EVA thin film face-to-face and sent into a thermal laminator for heat sealing. The photoluminescense measurement of the samples is recorded by a fluorescence spectrometer (EI/FL S980-S2S2-STM) with a Xe lamp at room temperature. Otherwise, home-made measuring equipment is built to measure MIE properties for the pressure sensor devices. A ballpoint is fixed on a linear motor to apply periodic stress on the device by moving the pen. The dynamic spectra are collected from the force-bearing point of the devices via a spectrometer (Ocean Optics QE65pro) in the range of 200–900 nm. The output optical powers are measured by a power meter (Thorlabs PM100D) equipped with the probe (Thorlabs S120VC). In the meantime, the vertical contact force is measured by a stress sensor (ATI Nano17).

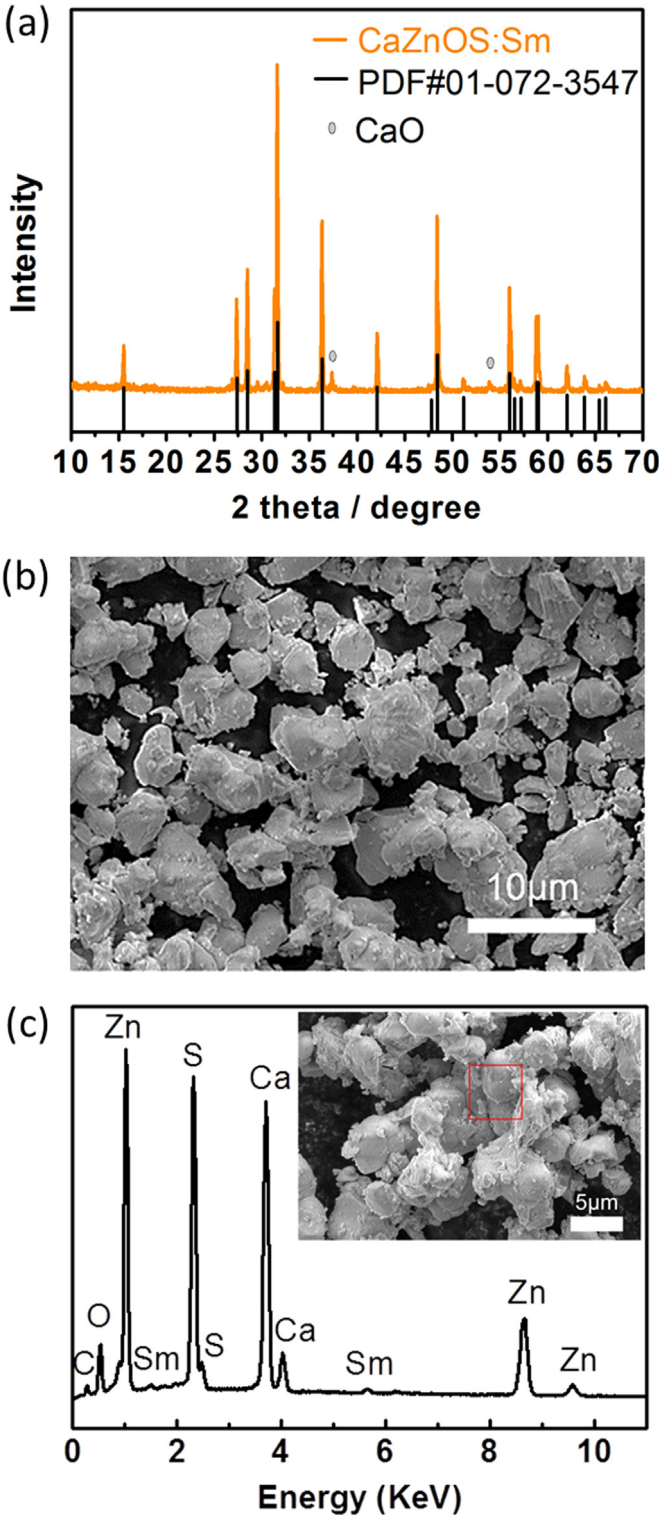

Fig. 1. Characterization of the CaZnOS:Sm^{3+} powders. (a) XRD pattern of the CaZnOS:Sm^{3+}sample. (b) The SEM images of CaZnOS:Sm^{3+}. (c) EDS spectrum of the CaZnOS:Sm^{3+} particles. (Illustration) a magnified SEM picture of the CaZnOS:Sm^{3+} pellet samples.

3. Results and analysis

The compositions and morphology of the CaZnOS:Sm^{3+}compounds are investigated. Fig. 1(a) shows the XRD pattern of the CaZnOS:Sm^{3+} doped sample and the CaZnOS standard pattern (PDF 01-072-3547) for comparison. The XRD results reveal that the synthesized CaZnOS:$Sm^{3+}$is composed of main CaZnOS phase combined with a small amount of CaO impurity, which is consistent with the previous report [13]. The ionic radii of Sm^{3+} (r=0.958 Å, CN=6) is similar to that of Ca^{2+} (r=1.00 Å, CN=6), but much larger than that of Zn^{2+} (r=0.6 Å, CN=4). Due to a compatable ionic radii, Sm^{3+} ions are doped into the host to substitute Ca site. The morphology of the doped CaZnOS powders

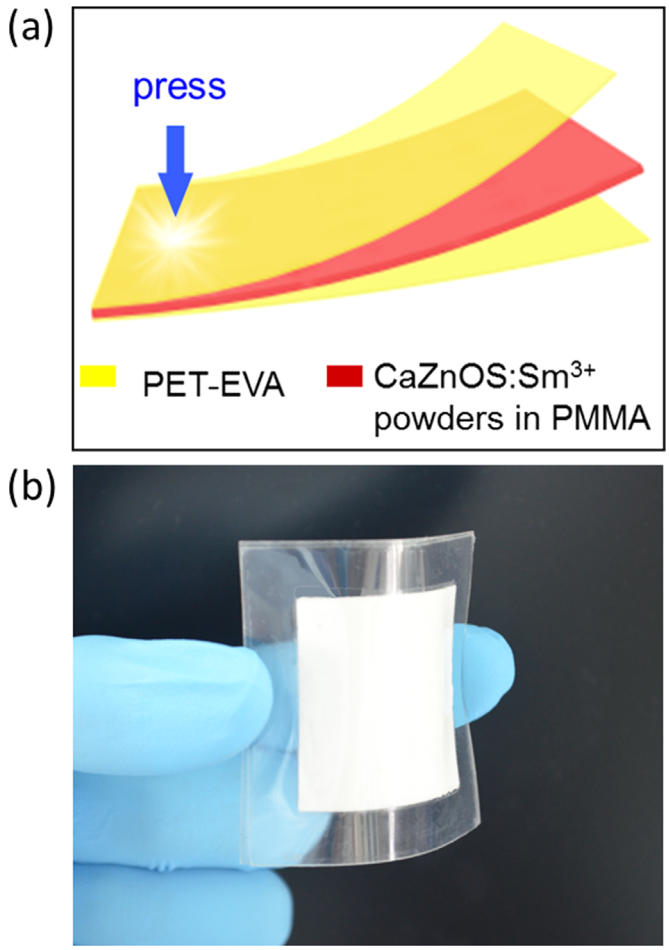

Fig. 2. (a) Schematic configuration of the flexible stress sensor device. (b) A photograph of the pressure sensor devices is demonstrated.

is examined by SEM (Fig. 2(b)). It can be clearly seen that the CaZnOS:Sm^{3+} phosphor powders are made up of spherical-like particles with size about 5 μm. Fig. 1(c) shows the energy dispersive spectrum (EDS), two small peaks of Sm are presented in the EDS data for the CaZnOS:Sm^{3+} sample. A little peak of C is observed due to the karbogel used during sample measurement.

For the investigation of the MIE properties of the doped piezosemiconductive powders, we prepare a flexible stress sensor device. Fig. 2(a) and (b) shows the schematic configuration and the real photograph of the flexible device respectively. As shown the pressure sensor devices with a sandwich-like structures are simplify constructed by the mix of CaZnOS:Sm^{3+} powders and PMMA in the middle layer, packaged by the PET-EVA film at top and bottom. It should be noted that the PMMA acts as the encapsulant that disperse and fix the CaZnOS:Sm^{3+} to form flexible composite particles. At the same time, the transparent PET-EVA as the protective films after heat sealing. All above, a flexible pressure sensor device is made for the further measurement.

Fig. 3 shows the mechanical-induced emission spectra of CaZnOS:Sm^{3+} under a writing force of 19 N. To investigate the origination of the stress-induced emission, the photoluminescence spectrum under 407 nm excitation is list as a comparison. As show in the figure MIE spectrum of CaZnOS:Sm^{3+} sample exhibits red emission which composed of peaks at about 566 nm, 580–623 nm, 653–673 nm and 712–735 nm, corresponding to the $^4G_{5/2} \rightarrow {}^6H_J$ (J=5/2,7/2, 9/2,and 11/2) transitions of Sm^{3+}, respectively. Comparably, the MIE spectrum matches well with the PL spectrum,

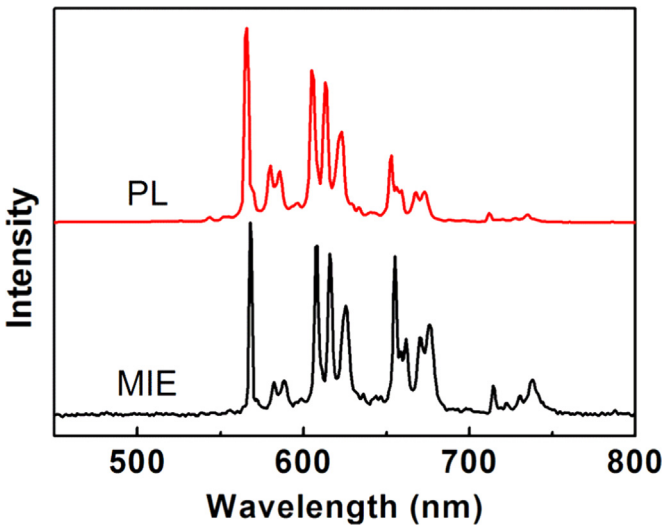

Fig. 3. Comparisons of photoluminescence (407 nm excitation) and mechanical-induced emission of CaZnOS:Sm^{3+}.

indicating that the MIE emission originates from the same luminescence center as PL.

The MIE features of these devices are researched by applying different pressures. A full MIE spectrum derived from a device under a series of loaded forces is shown in Fig. 4(a). The integral emission intensity which responds to each wavelength shows a unidirectional increase with increasing of the applied force. Once a moderate mechanical stress is applied on the film devices, for instance, slight scraping by a piece of thin glass slide, a bright and vivid red light emission is clearly observed by the naked eye even in the daylight. To evaluate the absolutely MIE intensity, the output optical powers are measured to be circa serial tens nano-watt by a power meter in our experimental condition under different pressures. In addition, the integral intensity versus external pressures is plotted in Fig. 4b, and the slope of the curve is defined as the sensitivity of the device, and has a good linearly increasing trend in the range of 13–65 MPa. As presented in the Fig. 4(c), we write “a b c” on a device and record this visible dynamic pressure process by an ordinary camera of a smart phone using specious software with a delay imaging capability. The MIE response time of the device is measured, the value is 10.01 ms. Given the time resolution of our spectrometer being 8 ms, the real response time of our devices can be much shorter than this value. Meantime, the corresponding 2D distribution of relative MIE intensity derived by extracting gray scale from Fig. 4(c) is shown in Fig. 4(d). It clearly demonstrates the intensity and distribution of the light emission. So, the stress information input during the writing process can be recorded and mapped by analyzing the intensity and distribution of the photograph.

The mechanism of mechanically-induced emission is also discussed. The optical band gap at room temperature of CaZnOS is estimated at 3.7 eV [19]. Besides, the charge transfer band of Sm^{3+} in CaZnOS is observed around 3.3 eV determines the position of the Sm 4f ground state with respect to the top of the valence band in Fig. 5(a) [22]. To date, several kinds of mechanisms have been proposed for the MIE process, while the piezoelectric potential plays an important role in the MIE process of CaZnOS [23]. The steps involved in the MIE process in CaZnOS:Sm^{3+} crystals are as follows Fig. 5(b): ① when a mechanical stress is applied, piezoelectric polarization charges will be induced due to the non-centrosymmetric characteristic of the crystal structure of CaZnOS, then the conduction and valance bands of CaZnOS are tilted under the potential generated by the piezo-charges; ② as a consequence, the trapped electrons in the upper electron defect state become

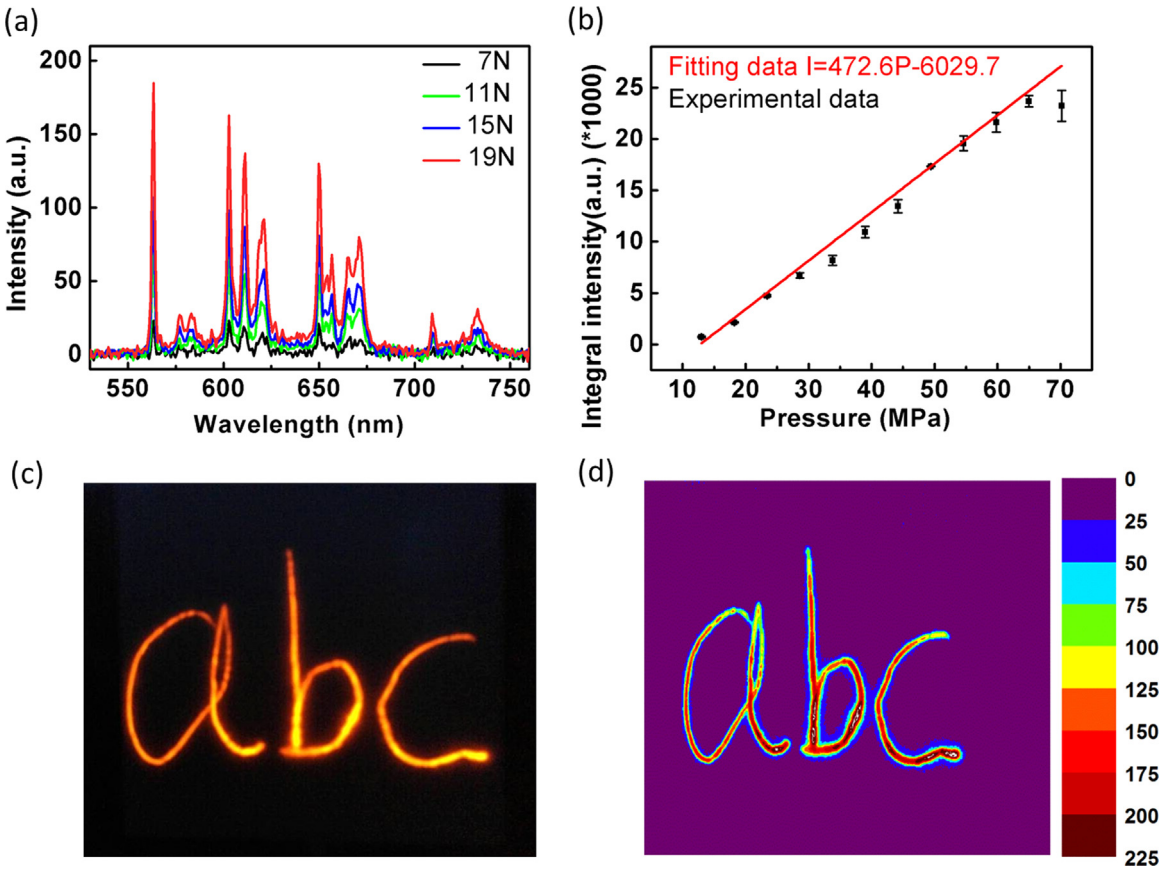

Fig. 4. (a) MIE spectra under different load for a pressure sensor device. (b) Integral intensity over 550–800 nm under a series of dynamic pressure with a pen of 0.7 mm diameter. (c) A handwriting "a b c" reflects the visualization of dynamic pressure distributions. (d) The gray scale is derived from (c) which is corresponding 2D distribution of relative MIE intensity.

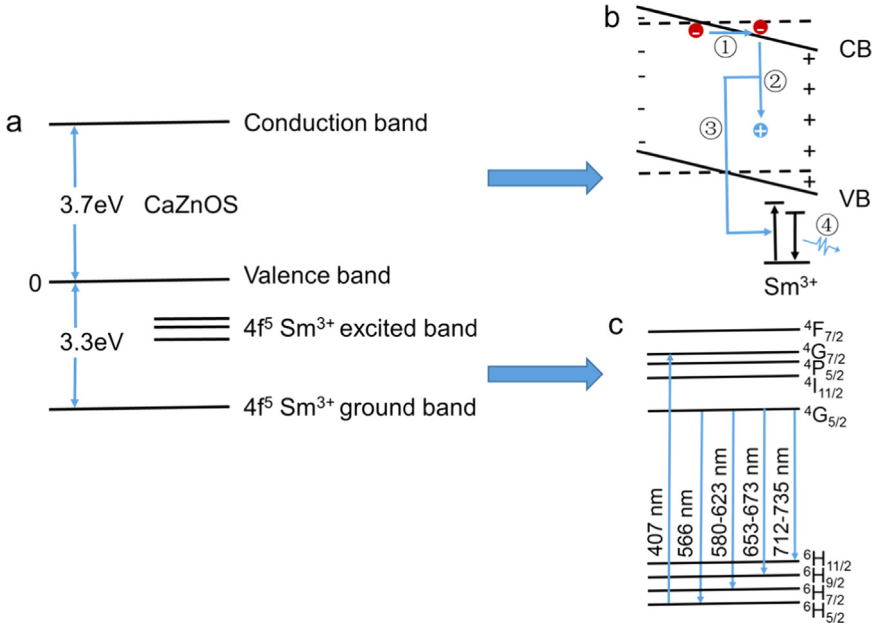

Fig. 5. The proposed mechanism of photoluminescence and mechanical-induced emission in the Sm^{3+} doped CaZnOS.

much easier to be detrapped or released into the conduction band of CaZnOS:Sm^{3+}; ③ release of energy non-radiatively during the electron–hole recombination and transfer energy to Sm^{3+}ions; ④ excited Sm^{3+}ions fall back to the ground state with red light emission. As presented in Fig. 5(c), the PL emissions process involve the 4f electrons of Sm^{3+} first nonradiatively relax to $^4G_{5/2}$ from the high level of $^4G_{7/2}$, and then recombine to lower levels of ^6H_J (J=5/2, 7/2, 9/2, 11/2) when the electrons are excited.

4. Conclusions

We report that the Sm^{3+}-doped CaZnOS piezoelectric

semiconductor shows strong red emission induced by mechanical stress. Under moderate mechanical stimuli, the doped samples exhibit strong visible red emission to the naked eyes even under the day light. Based on the prepared samples, a flexible pressure sensor device is fabricated and the mechanically-induced emission properties are studied. The spectrum of mechanically-induced emission is well agreement with the PL spectrum, suggesting they originate from the same luminescent center. The real-time pressure distribution is visualized and recorded through the obvious linear relationship between integrated MIE intensity and the applied pressure. Our results show that the lanthanide doped piezoelectric semiconductors could be applied into the flexible pressure sensor devices and provide the opportunities for applications in mapping of personalized handwriting, smart display, and human machine interface.

Acknowledgments

The authors are grateful for the support received from the Doctoral Foundation of Chongqing Normal University, China (Grant no. 10XLB001); the “thousand talents” program for the pioneer researcher and the innovation team in China, the Presidential Funding of the Chinese Academy of Sciences, the National Natural Science Foundation of China (No. 51272238, 21321062, 51432005, 51502018 and 61405040), and Beijing City Committee of Science and Technology (Z151100003315010).

Appendix A. Supplementary material

Supplementary data associated with this article can be found in the online version at http://dx.doi.org/10.1016/j.optcom.2016.03.046.

References

[1] N. Wang, C.Z. Gao, F. Xue, Y. Han, T. Li, X. Cao, X.J. Zhang, Y. Zhang, Z.L. Wang, ACS Nano 9 (3) (2015) 3159.
[2] R.M. Yu, C.F. Pan, Z.L. Wang, Energy Environ. Sci. 6 (2) (2013) 494.
[3] C.F. Wang, R.R. Bao, K. Zhao, T.P. Zhang, L. Dong, C.F. Pan, Nano Energy 14 (2015) 364.
[4] Q. Yang, Y. Liu, C.F. Pan, J. Chen, X.N. Wen, Z.L. Wang, Nano Lett. 13 (2) (2013) 607.
[5] W.Z. Wu, X.N. Wen, Z.L. Wang, Science 340 (6135) (2013) 952.
[6] C.F. Pan, L. Dong, G. Zhu, S.M. Niu, R.M. Yu, Q. Yang, Y. Liu, Z.L. Wang, Nat. Photonics 7 (9) (2013) 752.
[7] N. Terasaki, H. Zhang, H. Yamada, C.N. Xu, Chem. Commun. 47 (28) (2011) 8034.
[8] B.P. Chandra, V.K. Chandra, P. Jha, Appl. Phys. Lett. 104 (3) (2014) 031102.
[9] S. Kamimura, H. Yamada, C.N. Xu, Appl. Phys. Lett. 101 (9) (2012) 091113.
[10] Y. Fujio, C.N. Xu, M. Nishibori, Y. Teraoka, K. Kamitani, N. Terasaki, N. Ueno, J. Adv. Dielectr. 04 (02) (2014) 1450016.
[11] S.M. Jeong, S. Song, S.K. Lee, N.Y. Ha, Adv. Mater. 25 (43) (2013) 6194.
[12] Y. Zhang, G.Y. Gao, Helen L.W. Chan, J.Y. Dai, Y. Wang, J.H. Hao, Adv. Mater. 24 (13) (2012) 1729.
[13] J.C. Zhang, C.N. Xu, S. Kamimura, Y. Terasawa, H. Yamada, X.S. Wang, Opt. Express 21 (11) (2013) 12976.
[14] X.S. Wang, C.N. Xu, H. Yamada, K. Nishikubo, X.G. Zheng, Adv. Mater. 17 (10) (2005) 1254.
[15] N. Terasaki, H. Yamada, C.N. Xu, Catal. Today 201 (2013) 203.
[16] X.D. Wang, H.L. Zhang, R.M. Yu, L. Dong, D.F. Peng, A.H. Zhang, Y. Zhang, H. Liu, C.F. Pan, Z.L. Wang, Adv. Mater. 27 (14) (2015) 2324.
[17] D.F. Peng, B. Chen, F. Wang, Chempluschem 80 (8) (2015) 1209.
[18] S.L. Gai, C.X. Li, P.P. Yang, J. Lin, Chem. Rev. 114 (4) (2014) 2343.
[19] T. Sambrook, C.F. Smura, S.J. Clarke, K.M. Ok, P.S. Halasyamani, Inorg. Chem. 46 (7) (2007) 2571.
[20] H.P. Wagner, M. Kuhnelt, W. Langbein, J.M. Hvam, Phys. Rev. B 58 (16) (1998) 10494.
[21] D. Tu, C.N. Xu, Y. Fujio, S. Kamimura, Y. Sakata, N. Ueno, Appl. Phys. Lett. 105 (1) (2014) 011908.
[22] Z.J. Zhang, A. Feng, X.Y. Chen, J.T. Zhao, J. Appl. Phys. 114 (21) (2013) 213518.
[23] H.L. Zhang, D.F. Peng, W. Wang, L. Dong, C.F. Pan, J. Phys. Chem. C 119 (50) (2015) 28136.